Performance Analysis of Diffusion Filtered-X Algorithms in Multitask ANC Systems

Y. J. Chu
State Key Laboratory of Subtropical Building Science, South China University of Technology
Guangzhou, China
chuyj@scut.edu.cn

S. C. Chan
Dept. Electrical Electronics Engineering,
The University of Hong Kong,
Hong Kong
scchan@eee.hku.hk

Y. Zhao
State Key Laboratory of Subtropical Building Science, South China University of Technology
Guangzhou, China
arzhyzh@scut.edu.cn

M. Wu
Key Laboratory of Noise and Vibration Research,
Institute of Acoustics,China
Bejing, China
mingwu@mail.ioa.ac.cn

***Abstract*—The centralized control for multi-channel active noise control (ANC) systems usually cost considerable processing power due to the transfer functions between a large number of loudspeakers and error microphones; while the decentralized control has the increased risk of global instability. Distribution of the controller network could save computational burden while maintaining satisfactory performance. A lot of ANC algorithms employing diffusion control have been proposed recently. The communication within diffusion networks introduces the estimation bias of each controller and makes it difficult to analyze the performance of the entire system. This paper analyzes the performance of the diffusion ANC network based on a family of diffusion filtered-x (Fx) algorithms employing either the single- or multiple-measurement. Difference equations describing the mean and mean squares convergence behaviors of these ANC systems are derived to characterize its optimal solution, estimation bias and variance. Simulations have been conducted to compare the performance of diffusion Fx algorithms and the effectiveness of the theoretical analysis.**

Keywords—active noise control (ANC), diffusion control, multitask problem, and performance analysis

I. INTRODUCTION

Active control of noise usually involves a large number of loudspeakers and error microphones in order to achieve the global control over a region of space [1]. As shown in Fig. 1, the noisy signal $\{x(n)\}$ is picked up by a microphone located near the noise source. In order to create a quiet zone, the K-node undesirable sound $\{d_{0k}(n)\}$ for $k = 1,\ldots, K$, should be cancelled by the acoustic signal $\{y_k(n)\}$ generated from a loudspeaker through an adaptive controller $\{w_k(n)\}$. One of the most widely used active noise control (ANC) algorithms is the filtered-x (Fx) algorithm [2]. The error microphone is used to pick up the error signal $\{e_k(n)\}$ to be minimized by Fx algorithms. The acoustic path from source to microphones, called the primary path, is modeled as a finite impulse response (FIR) $\{h_k(n)\}$; and the path from the ith loudspeaker to jth microphone, called the secondary path, is modeled as FIRs $\{s_{ij}(n)\}$. $\{\hat{s}_{ij}(n)\}$ is the estimate. Only the kth secondary path has been shown in Fig. 1. The other secondary sources result in the interference $\{\gamma_k(n)\}$ at the kth microphone. $\{\eta_k(n)\}$ is the background noise rather than the noise source $\{x(n)\}$ to be cancelled.

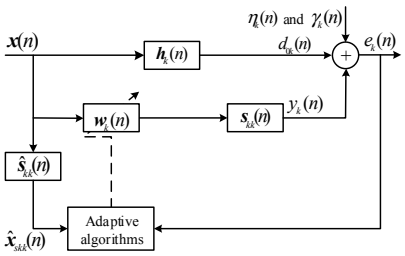

Fig. 1: Block diagram of the kth channel of a multi-channel ANC system using the Fx-based adaptive algorithm.

For multi-channel ANC systems, adaptive algorithms have been proved to perform very well for centralized processing [1]. An important issue in centralized control is the modeling of the secondary paths and the corresponding large computational burden. To reduce complexity and facilitate hardware of multi-channel control systems, the decentralized control has been developed [3]. It is capable of reducing the computational burden, but brings in the major drawback of the increased risk of global instability. A lot of effort has been taken to derive a sufficient stability condition for such systems [4]-[6]. Recently, a two-channel decentralized ANC algorithm is proposed that has a guaranteed convergence and good noise reduction [7]. As an alternative, distributed strategies are developed over multi-channel ANC networks [8]-[10]. These algorithms allow more channels and distribute computational complexity to all nodes. Meanwhile, an improved robustness is obtained due to the cooperation between nodes. This cooperative manner makes the performance analysis of the ANC system more complicated. In [11], the mean and the mean-square deviation performance of a distributed affine projection algorithm (APA) for ANC network is derived. This analysis is based on the assumption that the controller coefficients estimated at each node converge to the same value. The optimal solution to each controller, however, is barely the same [12], especially for networked ANC systems where error microphones are physically distributed in a large area, e.g., a full-sized open window or the surrounding of a large and noisy factory machine. This multitask problem in distributed networks is caused by the network topology [13]. Multitask problems in multichannel ANC systems is further explained in Section II. To our best knowledge, a detailed performance analysis on important issues

978-9-0827-9703-9/19/$31.00 ©2019 IEEE

in ANC networks, such as effect of networks on ANC systems and convergence conditions, is unavailable in current literature. Driven by practical advantages of network ANC systems, this paper is devoted to bridge this gap.

In this paper, the diffusion multi-channel ANC system is studied and a family of diffusion (Diff-) Fx algorithms, with either single or multiple measurement, are formulated. Moreover, performance of these Diff-Fx algorithms is studied and difference equations describing the mean and mean squares convergence behaviors are derived, which shows the effect of adaptive networks on the multitask ANC system. Simulations are conducted to verify the effectiveness of the theoretical analysis and compare the performance of Diff-Fx algorithms.

II. Review of the Diff-Fx Adaptive Algorithms

According to Fig. 1, the error signal at the *k*th microphone (or node) for $k = 1,\ldots, K$ receives the unwanted noise $d_k(n)$ and the output of the *k*th loudspeaker, which reads

$$e_k(n) = d_k(n) + y_k(n). \tag{1}$$

The noise signal $d_k(n)$ contains the undesirable sound $\{d_{0k}(n)\}$ at the *k*th node (the noise source $\{x(n)\}$ transferring through the *k*th primary path $h_k(n)$), the Gaussian random noise $\eta_k(n)$, and the interference $\gamma_k(n)$ from the secondary sources except the *k*th loudspeaker, which can be expressed as

$$d_k(n) = d_{0k}(n) + \eta_k(n) + \gamma_k(n) \tag{2}$$

where we define the discrete time convolution "*" such that $d_{0k}(n) = h_k(n) * x(n)$, $\gamma_k(n) = \sum_{l\neq k, l=1}^{K} x(n) * w_l(n) * s_{lk}(n)$, and signal from the *k*th loudspeaker can be written as $y_k(n) = x(n) * w_k(n) * s_{kk}(n)$.

The controller $\{w_k(n)\}$ aims to minimize the power of $\{e_k(n)\}$. To this end, we collect the multiple measurement vector $\boldsymbol{e}_k(n)$ and the filtered input matrix $\hat{\boldsymbol{X}}_k(n)$

$$\boldsymbol{e}_k(n) = [e_k(n),\ldots,e_k(n-M+1)]^T \ (M\times 1)$$
$$\hat{\boldsymbol{X}}_k(n) = [\hat{\boldsymbol{x}}_k(n),\ldots,\hat{\boldsymbol{x}}_k(n-M+1)] \ (L\times M)$$

where $\hat{\boldsymbol{x}}_k(n) = [\hat{x}_{skk}(n),\ldots,\hat{x}_{skk}(n-L+1)]^T$ is the filtered input vector with $\hat{x}_{slk}(n) = x(n) * \hat{s}_{lk}(n)$ (l, $k = 1,\ldots, K$), *M* is the project number, and *L* the length of adaptive filter for the ANC controller $\{w_k(n)\}$. Then, we seek the solutions to the controller that minimizes the following cost function ε_k

$$\varepsilon_k = E[\boldsymbol{e}_k^T(n)\boldsymbol{P}_k(n)\boldsymbol{e}_k(n)] \tag{3}$$

where $\boldsymbol{P}_k(n) = E[\hat{\boldsymbol{X}}_k^T(n)\hat{\boldsymbol{X}}_k(n) + \xi\boldsymbol{I}_M]^{-1}$ [14] is the projection matrix with ξ a small positive parameter, namely the regularization parameter, and $\boldsymbol{I}_M$ the $M \times M$ identity matrix. It should be noted that as a special case of the projection matrix, if $M = 1$, Eq. (3) leads to Diff-Fx Normalized LMS (Diff-Fx-NLMS) algorithm; if $\boldsymbol{P}_k(n)$ is an identity matrix, Eq. (3) represents the Diff-FxLMS algorithm [15].

Each node has an access to a set of local estimates $\{\boldsymbol{\psi}_k(n)\}$ of ANC controllers within a neighborhood, say $\mathcal{N}_k$, which is connected to node *k* by an edge. The local estimates are then fused at node *k* over the neighborhood $l \in \mathcal{N}_k$ through combination weights a_{lk}, which satisfy $\sum_{l\in\mathcal{N}_k} a_{lk} = 1$. Then, the Fx algorithm that uses a Combine Then Adapt (CTA) diffusion strategy, namely the CTA-Fx- algorithm, and minimizes the instantaneous MSE (3) at node *k* can be summarized as

$$\boldsymbol{w}_k(n) = \sum_{l\in\mathcal{N}_k} a_{lk}\boldsymbol{\psi}_l(n) \tag{4}$$

$$\begin{aligned}\boldsymbol{\psi}_k(n+1) &= \boldsymbol{w}_k(n) - \tfrac{1}{2}\mu_k\nabla\varepsilon_k(n)\\ &= \boldsymbol{w}_k(n) - \mu_k\hat{\boldsymbol{X}}_k(n)\boldsymbol{P}_k(n)\boldsymbol{e}_k(n)\end{aligned} \tag{5}$$

where $\mu_k > 0$ is the local step-size. Note, the contribution of the true filtered signal to $\{e_k(n)\}$ is denoted as $\{x_{skk}(n)\}$, which forms the matrix $\boldsymbol{X}_k(n)$ and vector $\boldsymbol{x}_k(n)$ of the same structure, respectively, with $\hat{\boldsymbol{X}}_k(n)$ and $\hat{\boldsymbol{x}}_k(n)$. It can be seen from (4)(5) that the controller is updated in a cooperative way within the network and combined according to a certain network topology. This changes the optimal solution to each node that approximates $\{-h_k(n)\}$ after cascading with $\{s_{kk}(n)\}$ [12]. Solutions deviate significantly if the nodes are located far away. This results in the multitask problem in ANC networks.

III. Performance Analysis

In this section, the performance of the proposed Diff-Fx based algorithms with Gaussian inputs and additive white Gaussian noise is analyzed. Since it is a multitask problem [13], i.e., each controller converges to different optimal solutions, it is rather challenging to study the performance of the networked ANC controller. Several assumptions are hence adopted in order to make the analysis tractable and gain insight into the behavior of these adaptive algorithms.

The assumptions made to facilitate the performance analysis are as follows:

(A1) $\{\hat{x}_{sij}(n)\}$ is the zero-mean Gaussian random signals;

(A2) $\boldsymbol{x}_k(n)$ is independent with $\boldsymbol{w}_k(n)$ and $\eta_k(n)$; so is the estimated filtered input $\hat{\boldsymbol{x}}_k(n)$;

(A3) the interference $\{\gamma_k(n)\}$ is independent with the filtered input $\{x_{skk}(n)\}$.

We then define the following global representations for the stochastic quantities that appear in the update equations (4) and (5), respectively, for the global and local estimates

$$\boldsymbol{\psi}_C(n) = \mathrm{col}\{\boldsymbol{\psi}_1(n),\ldots,\boldsymbol{\psi}_K(n)\},\ \boldsymbol{w}_C(n) = \mathrm{col}\{\boldsymbol{w}_1(n),\ldots,\boldsymbol{w}_K(n)\},$$
$$\boldsymbol{e}(n) = \mathrm{col}\{\boldsymbol{e}_1(n),\ldots,\boldsymbol{e}_K(n)\},\ \boldsymbol{\mathcal{X}}(n) = \mathrm{diag}\{\boldsymbol{X}_1(n),\ldots,\boldsymbol{X}_K(n)\},$$

and $\hat{\boldsymbol{\mathcal{X}}}(n) = \mathrm{diag}\{\hat{\boldsymbol{X}}_1(n),\ldots,\hat{\boldsymbol{X}}_K(n)\}$. The filter vectors have a length of *LK*, the error vector has *MK* elements, while the input matrices are of size $(LK \times MK)$.

Using the above representations, the measurements in (1) are

assumed to obey a linear model as

$$\boldsymbol{e}(n) = \boldsymbol{d}(n) + \boldsymbol{\mathcal{X}}^T(n)\boldsymbol{w}_C(n) \tag{6}$$

where $\boldsymbol{d}(n) = \text{col}\{\boldsymbol{d}_1(n),...,\boldsymbol{d}_K(n)\}$ is a vector of size MK. It contains the vector $\boldsymbol{d}_k(n) = [d_k(n),...,d_k(n-M+1)]^T$ of length M as the kth element.

The block diagonal matrix of dimension $LK \times LK$ that collects the local step-sizes is defined as

$$\boldsymbol{D}_\mu(n) = \text{diag}\{\mu_1\boldsymbol{I}_L,...,\mu_K\boldsymbol{I}_L\}$$

while the block diagonal matrix of dimension $MK \times MK$ collects the inverse of the covariance matrix as

$$\boldsymbol{\mathcal{P}}(n) = [\hat{\boldsymbol{\mathcal{X}}}^T(n)\hat{\boldsymbol{\mathcal{X}}}(n) + \xi\boldsymbol{I}_{MK}]^{-1} = \text{diag}\{\boldsymbol{P}_1(n),...,\boldsymbol{P}_K(n)\}.$$

Using these definitions, we hence have the following global representation from (5)

$$\boldsymbol{\psi}_C(n+1) = \boldsymbol{\psi}_G(n) - \boldsymbol{D}_\mu\hat{\boldsymbol{\mathcal{X}}}(n)\boldsymbol{\mathcal{P}}(n)\boldsymbol{e}(n) \tag{7}$$

where $\boldsymbol{\psi}_G(n) = \boldsymbol{G}\boldsymbol{\psi}_C(n)$, $\boldsymbol{G} = \boldsymbol{A}^T \otimes \boldsymbol{I}_L$ is the $LK \times LK$ network topology matrix with $\otimes$ the Kronecker product and the combining matrix $\boldsymbol{A}$ formed by $\{a_{lk}\}$ for $l, k = 1,\ldots,K$. Without the loss of generality, we assume a symmetric combining matrix such that we have $\boldsymbol{G} = \boldsymbol{G}^T$.

A. Mean Convergence Analysis

We assume that the algorithm is convergent such that $\boldsymbol{\psi}_C(n)$ converges to $\boldsymbol{\psi}_\infty$ at the steady state. Then the solution $\boldsymbol{\psi}_\infty$ finds from (7) as

$$\boldsymbol{\psi}_\infty = -[\boldsymbol{R}_{\hat{X}X}\boldsymbol{G} + \boldsymbol{D}_\mu^{-1}(\boldsymbol{I}_{LK} - \boldsymbol{G})]^{-1}\boldsymbol{r}_{\hat{X}d} \tag{8}$$

where $\boldsymbol{R}_{\hat{X}X} = E[\hat{\boldsymbol{\mathcal{X}}}(n)\boldsymbol{\mathcal{P}}(n)\boldsymbol{\mathcal{X}}^T(n)]$ is the covariance matrix, and $\boldsymbol{r}_{\hat{X}d} = E[\hat{\boldsymbol{\mathcal{X}}}(n)\boldsymbol{\mathcal{P}}(n)\boldsymbol{d}(n)]$ is the cross-correlation vector.

It can be seen from (8) that the multitask problem introduces an extra bias term (the second term in the brackets) through the network topology such that $\boldsymbol{\psi}_k(n)$ converges to different steady-state values and the relationship $\boldsymbol{\psi}_\infty = \boldsymbol{G}\boldsymbol{\psi}_\infty$ no longer holds. This means the assumption that all nodes converge to the same value is not true in multichannel ANC systems. Furthermore, the deviation, $\Delta\boldsymbol{\psi} = \boldsymbol{\psi}_0 - \boldsymbol{\psi}_\infty$, from the Winner solution $\boldsymbol{\psi}_0 = -(\boldsymbol{R}_{\hat{X}X}\boldsymbol{G})^{-1}\boldsymbol{r}_{\hat{X}d}$ can be found from (8)

$$\boldsymbol{R}_{\hat{X}X}\boldsymbol{G}\Delta\boldsymbol{\psi} = \boldsymbol{D}_\mu^{-1}(\boldsymbol{I}_{LK} - \boldsymbol{G})\boldsymbol{\psi}_\infty \tag{9}$$

which is introduced by the network topology [13].

We then obtain from (5) the following mean difference equation and examine its convergence rate

$$\bar{\boldsymbol{v}}(n+1) = [\boldsymbol{I}_{LK} - \boldsymbol{D}_\mu\boldsymbol{R}_{\hat{X}X}]\bar{\boldsymbol{v}}_G(n) \tag{10}$$

where $\bar{u}$ denotes $E[u]$, $\boldsymbol{v}(n) = \boldsymbol{\psi}_\infty - \boldsymbol{\psi}_C(n)$, $\boldsymbol{v}_G(n) = \boldsymbol{G}\boldsymbol{v}(n)$.

From (10), we find the mean weight vector converges if

$$|\lambda\{[\boldsymbol{I}_{LK} - \boldsymbol{D}_\mu\boldsymbol{R}_{\hat{X}X}]\boldsymbol{G}\}| < 1 \tag{11}$$

where $\lambda\{\cdot\}$ denotes the eigenvalues of a given matrix.

B. Mean Squares Convergence Analysis

We first derive a difference equation for covariance matrices $\boldsymbol{\Xi}(n) = E[\boldsymbol{v}(n)\boldsymbol{v}^T(n)]$, and $\boldsymbol{\Xi}_G(n) = E[\boldsymbol{v}_G(n)\boldsymbol{v}_G^T(n)]$

To have a concise expression in the following analysis, the signals are represented by using the following column vectors of size ($MK \times 1$):

$$\boldsymbol{d}_0(n) = \text{col}\{\boldsymbol{d}_{01}(n),...,\boldsymbol{d}_{0K}(n)\},$$
$$\boldsymbol{\eta}_C(n) = \text{col}\{\boldsymbol{\eta}_1(n),...,\boldsymbol{\eta}_K(n)\},$$
$$\boldsymbol{\gamma}_C(n) = \text{col}\{\boldsymbol{\gamma}_1(n),...,\boldsymbol{\gamma}_K(n)\},$$

where the kth element of the abovementioned vectors are vectors of length M, i.e.,

$$\boldsymbol{d}_{0k}(n) = [d_{0k}(n),...,d_{0k}(n-M+1)]^T,$$
$$\boldsymbol{\eta}_k(n) = [\eta_k(n),...,\eta_k(n-M+1)]^T,$$
$$\boldsymbol{\gamma}_k(n) = [\gamma_k(n),...,\gamma_k(n-M+1)]^T.$$

Accordingly, Eq. (6) can be rewritten as

$$\boldsymbol{e}(n) = -\boldsymbol{\mathcal{X}}^T(n)\boldsymbol{G}(\boldsymbol{\psi}_0 - \boldsymbol{\psi}_C(n)) + \boldsymbol{\eta}_\Sigma(n) \tag{12}$$

where $\boldsymbol{\eta}_\Sigma(n) = \boldsymbol{\eta}_C(n) + \boldsymbol{\gamma}_C(n) + \boldsymbol{\Delta}_\Sigma(n)$ and $\boldsymbol{\Delta}_\Sigma(n) = \boldsymbol{d}_0(n) + \boldsymbol{\mathcal{X}}^T(n)\boldsymbol{w}_0$ is the modeling error typical for Fx algorithms.

Using the expressions in (12), we have from (5)

$$\begin{aligned}\boldsymbol{\Xi}(n+1) &= \boldsymbol{\Xi}_G(n) - \boldsymbol{D}_\mu\boldsymbol{R}_{\hat{X}X}\boldsymbol{\Xi}_G(n) - \boldsymbol{\Xi}_G(n)\boldsymbol{R}_{X\hat{X}}\boldsymbol{D}_\mu \\ &+ \boldsymbol{D}_\mu\boldsymbol{R}_{\hat{X}X}\boldsymbol{v}_G(n)\boldsymbol{\psi}_\infty^T(\boldsymbol{G}-\boldsymbol{I}_{LK})^T + (\boldsymbol{G}-\boldsymbol{I}_{LK})\boldsymbol{\psi}_\infty\boldsymbol{v}_G^T(n)\boldsymbol{R}_{X\hat{X}}\boldsymbol{D}_\mu \\ &+ \boldsymbol{D}_\mu E[\boldsymbol{Q}(n) - \boldsymbol{R}_\psi]\boldsymbol{D}_\mu\end{aligned} \tag{13}$$

where $\boldsymbol{R}_\psi = \boldsymbol{D}_\mu^{-1}(\boldsymbol{I}_{LK} - \boldsymbol{G})\boldsymbol{\psi}_\infty\boldsymbol{\psi}_\infty^T(\boldsymbol{I}_{LK} - \boldsymbol{G})^T\boldsymbol{D}_\mu^{-1}$, and

$$\boldsymbol{Q}(n) = E[\hat{\boldsymbol{\mathcal{X}}}(n)\boldsymbol{\mathcal{P}}(n)\boldsymbol{e}(n)\boldsymbol{e}^T(n)\boldsymbol{\mathcal{P}}(n)\hat{\boldsymbol{\mathcal{X}}}^T(n)]. \tag{14}$$

Eq. (14) contains the terms related to $\boldsymbol{\Xi}_G(n)$ and the driving terms; and $\boldsymbol{R}_\psi$ indicates the effect of diffusion topology. To investigate the dynamic of the difference equation, it is crucial to separate the terms related to $\boldsymbol{\Xi}_G(n)$ from (14). In this paper, Eq. (14) is first evaluated for a specified case of the Diff-Fx family, i.e., the Diff-FxLMS, and the following notations has been defined for $\boldsymbol{\mathcal{P}}(n) = \boldsymbol{I}$

$$\boldsymbol{Q}_\Xi(n) = 2\boldsymbol{R}_{\hat{X}X}\boldsymbol{\Xi}_G(n)\boldsymbol{R}_{X\hat{X}} + \boldsymbol{R}_{\hat{X}\hat{X}}Tr(\boldsymbol{\Xi}_G(n)\boldsymbol{R}_{XX}). \tag{15}$$

where $\boldsymbol{R}_{\hat{X}\hat{X}} = E[\hat{\boldsymbol{\mathcal{X}}}(n)\hat{\boldsymbol{\mathcal{X}}}^T(n)]$.

Consequently, Eq. (13) can be written as

$$\begin{aligned}\boldsymbol{\Xi}(n+1) &= \boldsymbol{\Xi}_G(n) - \boldsymbol{D}_\mu\boldsymbol{R}_{\hat{X}X}\boldsymbol{\Xi}_G(n) - \boldsymbol{\Xi}_G(n)\boldsymbol{R}_{X\hat{X}}\boldsymbol{D}_\mu \\ &+ \boldsymbol{D}_\mu(\boldsymbol{Q}_\Xi(n) + \boldsymbol{D}_\Sigma\boldsymbol{R}_{XX})\boldsymbol{D}_\mu + \boldsymbol{D}_\mu(\boldsymbol{R}_\psi + \tilde{\sigma}_\psi^2\boldsymbol{R}_{\hat{X}\hat{X}})\boldsymbol{D}_\mu\end{aligned}$$

$$+\boldsymbol{D}_{\mu}(\boldsymbol{R}_{\hat{X}X}\boldsymbol{\Xi}_{\Sigma,G}(n)\boldsymbol{R}_{X\hat{X}}+Tr(\boldsymbol{\Xi}_{\Sigma,G}(n)\boldsymbol{R}_{XX})\boldsymbol{R}_{\hat{X}\hat{X}})\boldsymbol{D}_{\mu} \quad (16)$$

where $\boldsymbol{D}_{\Sigma}=\mathrm{diag}\{\sigma_{\Sigma,1}^2\boldsymbol{I}_L,...,\sigma_{\Sigma,K}^2\boldsymbol{I}_L\}$, $\boldsymbol{R}_{XX}=E[\boldsymbol{\mathcal{X}}(n)\boldsymbol{\mathcal{X}}^T(n)]$, $\widetilde{\sigma}_{\psi}^2=Tr(\boldsymbol{R}_{XX}^{-1}\boldsymbol{R}_{\psi})$, and $\boldsymbol{\Xi}_{\Sigma,G}(n)=\bar{\boldsymbol{v}}_G(n)\Delta\boldsymbol{\psi}^T\boldsymbol{G}+\boldsymbol{G}^T\Delta\boldsymbol{\psi}\bar{\boldsymbol{v}}_G^T(n)$ which contains the mean error vector.

IV. Simulation Results

In this section, computer simulations are conducted to study the performance of the multi-channel ANC system using different diffusion adaptive filtering algorithms. The theoretical results are also evaluated.

A. Performance Analysis

In this experiment, the mean and mean squares performance analysis as shown, respectively, in (8) and (16) is examined. In this short paper, only the Diff-FxLMS algorithm is evaluated.

The primary path is generated randomly as FIR filters. To evaluate the theoretical results, a short primary path of length 10 is considered. They are randomly distributed on a circle of radius r centered at $\boldsymbol{h}_0$, i.e., $\boldsymbol{h}_i=\boldsymbol{h}_0+r\boldsymbol{g}_i$, for i = 1, …, 9, with $\boldsymbol{g}_i$ a Gaussian sequence of unit norm. The length of the controllers is also set to be 10. The secondary path has a length of 2. They are well estimated such that $\{\hat{x}_{slk}(n)\}$ is identical to $\{x_{slk}(n)\}$. The source noise is a Gaussian process. The variances of $\{d_{0k}(n)\}$ at each node are unit. The signal to noise ratios (SNRs) at each receiver is set to 20 dB. A 10-node ANC network is considered and a 10-by-10 combining Metropolis matrix with coefficients [0.1667, 0.2, 0.25, 0.3833, 0.4167, 0.4667, 0.5, 0.8333] is used as the combining matrix.

First, we verify the optimal solution of the Diff-FxLMS algorithm (8) in Fig. 2. Two measures are used, i.e., the weight-error vector with respect to 1) the Wiener solution: $\boldsymbol{v}^0(n)=\boldsymbol{G}[\overline{\boldsymbol{\psi}}_C(n)-\boldsymbol{\psi}_0]$ and 2) the optimal solution $\boldsymbol{v}^{Inf}(n)=\boldsymbol{G}[\overline{\boldsymbol{\psi}}_C(n)-\boldsymbol{\psi}_{\infty}]$. The radius r is set to 0, 0.05, and 0.1 to form the multitask problem. The step-size is set to 0.01. The Wiener solution curves (dash-dot lines) converge to a higher steady-state value as the radius increases. The optimal solution curves (solid lines) converge to a similar value, which is comparable to the Wiener solution curve at r = 0 (the one dash-dot line overlaps with 3 solid lines). It can be seen that for multitask problem, the controllers converge to the optimal solution in (8) rather than the Wiener solution that has identical values for each node.

In Fig. 3, the mean squares performance analysis in (16) is verified. The settings are identical to those in the previous experiment. It can be seen that the theoretical and simulated average excess MSE (EMSE) curves agree well with each other. It also shows that as the value of r increases, i.e., the optimal solution to each node becomes more different from each other, the estimation error will increase slightly.

B. Comparison of Different Diff-Fx- Algorithms

In this experiment, the Diff-Fx- algorithms are compared with each other. The algorithms under test include the CTA-FxLMS, CTA-FxNLMS, and CTA-FxAPA. Both white and colored noise sources are considered and their variances are normalized. For the colored input, a first order autoregressive (AR) process is considered, i.e., $x(n) = 0.5x(n–1) + v(n)$, where $v(n)$ is zero-mean and Gaussian distributed. For both white and colored noise sources, the step-sizes of the aforementioned algorithms are chosen as μ_{LMS} = 0.0002, μ_{NLMS} = 0.0015, and μ_{APA} = 0.001, respectively, so as to achieve similar steady-state EMSEs. For the CTA-FxAPA, the projection number is set to M = 3. The other settings are identical to those in the previous experiment.

The EMSE curves averaged over all nodes are shown in Fig. 4. It can be seen that when the noise source becomes colored, the CTA-FxLMS and CTA-FxNLMS algorithms converge at a much slower speed due to the spread eigenvalues of the input covariance matrix, while the CTA-FxAPA algorithm maintains fast convergence speed.

C. Comparison of Different Control Strategies

In this experiment, the control strategies under test include the centralized, decentralized, incrementally distributed, and diffusion control methods. We consider a scenario of noise control within an area of a 1.2 × 1.2 m square, say an open window in a building. A 10-channel ANC network is installed, i.e., 10 pairs of loudspeakers/microphones (a node) are installed. 8 nodes are installed on the edge and the distance between nodes is 0.5m. 2 nodes are located on the midline and 0.25m away from the center. Under this setting, the ANC system aims to cancel out the low frequency noise, say under 500 Hz. The primary path is generated with a fixed constraint such that it looks like a room impulse response. The length of the primary path is 150 (if the sampling rate is 1 KHz, the reverberation time is about hundreds of milliseconds). The radius r is set to 0, 0.01. The secondary path has a length of 8. The filter length is 150 and the step-sizes for the algorithms under test is 0.0003. The other settings are identical to those in the previous experiment.

The simulation results for the averaged EMSE curves are shown in Fig. 5. It can be seen that the incremental control has a higher steady-state residual level while the decentralized control increases the EMSE value gradually as the iteration. The diffusion control has a similar performance as the well-performed centralized control. Considering the computational cost of centralized control method, the diffusion control is more appropriate for practical use.

Conclusions

In this paper, the performance of a family of Diff-Fx adaptive algorithms has been studied. The effect of the diffusion strategies on the proposed algorithms in terms of the multitask solution, convergence speed and conditions, and steady-state estimation accuracy has been explored. The simulation results are found to be in good agreement with the theoretical predictions. The analysis provides useful insight of mechanism as well as guidance of design for the multi-channel ANC network algorithms.

Acknowledgment

This work was supported by the National Key Research and Development Program of China (2016YFB1200503), and National Natural Science Foundation of China under Grant No. 11474306, No. 11404367, No. 11474307.

REFERENCES

[1] S. Elliott, I. Stothers, and P. Nelson, "A multiple error LMS algorithm and its application to the active control of sound and vibration," IEEE Trans. Speech Signal Process., vol. 35, no. 10, 1423–1434, 1987.

[2] D. R. Morgan, "An analysis of multiple correlation cancellation loops with a filter in the auxiliary path," IEEE Trans. Acoust., Speech, Signal Process., ASSP-28(4), pp. 454–467, 1980.

[3] W. S. Levine, The Control Handbook, CRC Press, Boca Raton, 1996.

[4] T. Murao, J. He, B. Lam, R. Ranjan, C. Shi, and W. S. Gan, "Feasibility study on decentralized control system for active acoustic shielding," INTER-NOISE NOISE-CON Cong. Conf. Pro., InterNoise16, Hamburg Germany, 2016.

[5] L. Zhang, J. Tao, and X. Qiu, "Performance analysis of decentralized multi-channel feedback systems for active noise control in free space," Appl. Acoust., 74(1), 181–188, 2013.

[6] E. Leboucher, P. Micheau, A. Berry, and A. L'Espérance, "A stability analysis of a decentralized adaptive feedback active control system of sinusoidal sound in free space," J. Acoust. Soc. Am., vol. 111, pp. 189–199, Jan. 2002.

[7] G. Zhang, J. Tao, X. Qiu, and I. Burnett, "Decentralized two-channel active noise control for single frequency by shaping matrix eigenvalues," IEEE Trans. Audio, Speech, Lang. Process., 27, 44–52, 2019.

[8] M. Ferrer, M. de Diego, G. Piero, and A. Gonzalez, "Active noise control over adaptive distributed networks," Signal Process., vol. 107, pp. 82–95, 2015.

[9] J. M. Song and P. Park, "A diffusion strategy for the multichannel active noise control system in distributed network," Proc. 2016 Int. Conf. Computational Science and Computational Intelligence (CSCI2016), pp. 659–664, 2016.

[10] R. Kukde, G. Panda, and M. S. Manikandan, "On distributed non-linear active noise control using diffusion collaborative learning strategy," IET Signal Process., 12, pp. 410–421, 2018.

[11] M. Ferrer, A. Gonzalez, M. de Diego, and G. Piñero, "Distributed affine projection algorithm over acoustically coupled sensor networks," IEEE Trans. Signal Process., 65, pp. 6423–6434, 2017.

[12] S. C. Chan and Y. J. Chu, "Performance analysis and design of FxLMS algorithm in broadband ANC system with online secondary-path modeling," IEEE Trans. Audio, Speech, Lang. Process., vol. 20, no. 3, pp. 982–993, Mar. 2012.

[13] J. Chen, C. Richard, and A. Sayed, "Diffusion LMS over multitask networks," IEEE Trans. Signal Process., vol. 63, no. 11, pp. 2733–2748, 2015.

[14] M. Rupp, "Pseudo affine projection algorithms revisited: robustness and stability analysis," IEEE Trans. Signal Process., vol. 59, no. 5, pp. 2017–2023, May 2011.

[15] Y. J. Chu and C. M. Mak, "Diffusion control for multi-channel ANC systems using filtered-x algorithms," Pro. 24th Int. Cong. Sound Vib., London, UK, 23–27, Jul. 2017.

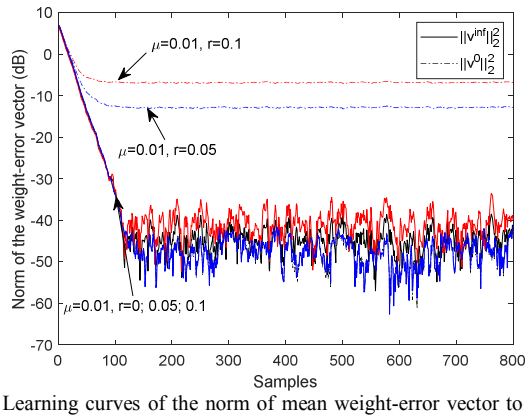

Fig. 2. Learning curves of the norm of mean weight-error vector to different solutions under different settings.

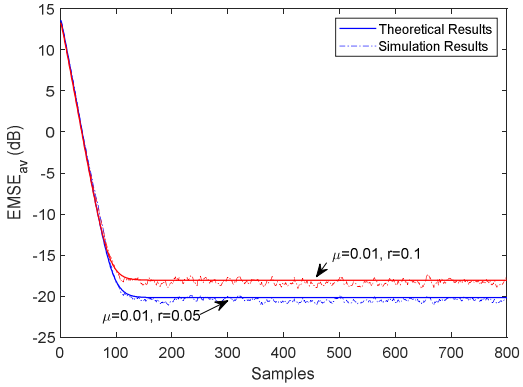

Fig. 3: Learning curves of EMSE using different radius values. μ_{LMS}=0.01.

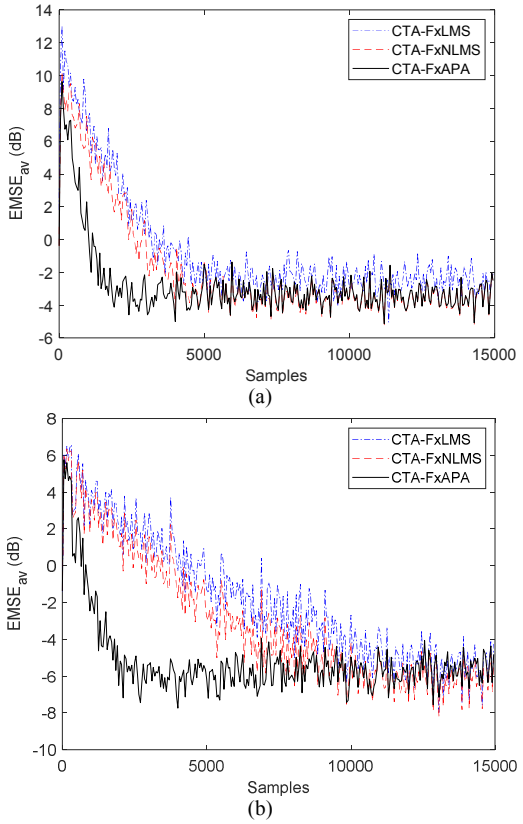

Fig. 4: Convergence curves of controllers using different Diff-Fx algorithms: (a) white noise sources; and (b) colored noise sources.

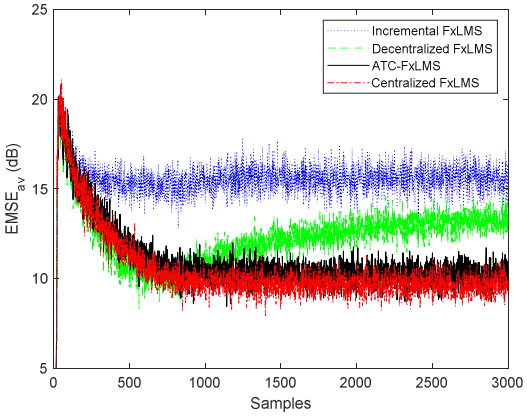

Fig. 5: Convergence curves of controllers using different control strategies.